Cyanides and Isocyanides of First-Row Transition Metals: Molecular Structure, Bonding, and Isomerization Barriers

Víctor M. Rayón,[†] Pilar Redondo,[†] Haydee Valdés,[‡] Carmen Barrientos,[†] and Antonio Largo*[,†]

Departamento de Química Física y Química Inorgánica, Facultad de Ciencias, Universidad de Valladolid, 47005 Valladolid, Spain, Center for Biomolecules and Complex Molecular Systems, Institute of Organic Chemistry and Biochemistry, Academy of Sciences of Czech Republic, 16610 Prague 6, Czech Republic

Received: March 28, 2007; In Final Form: May 17, 2007

Cyanides and isocyanides of first-row transition metal M(CN) (M = Sc−Zn) are investigated with quantum chemistry techniques, providing predictions for their molecular properties. A careful analysis of the competition between cyanide and isocyanide isomers along the transition series has been carried out. In agreement with the experimental observations, late transition metals (Co−Zn) clearly prefer a cyanide arrangement. On the other hand, early transition metals (Sc−Fe), with the only exception of the Cr(CN) system, favor the isocyanide isomer. The theoretical calculations predict the following unknown isocyanides, ScNC($^3\Delta$), TiNC($^4\Phi$), VNC($^5\Delta$), and MnNC($^7\Sigma^+$), and agree with the experimental observation of FeNC($^6\Delta$) and the CrCN($^6\Sigma^+$) cyanide. First-row transition metal cyanides and isocyanides are predicted to have relatively large dissociation energies with values within the range 80−101 kcal mol^{-1}, except Zn(CN), which has a dissociation energy around 50−55 kcal mol^{-1}, and low isomerization barriers. A detailed analysis of the bonding has been carried out employing the topological analysis of the charge density and an energy decomposition analysis. The role of the covalent and electrostatic contributions to the metal−ligand bonding, as well as the importance of π bonding, are discussed.

Introduction

The cyanide ion is one of the most interesting ligands in organometallic chemistry. Metal polycyanides are among the most studied complexes, with very well-known properties and applications. Besides, cyanogen (CN) is the simplest species in which carbon and nitrogen, two elements essential in the chemistry of life, appear combined in a molecule. Consequently, the study of the interaction between CN and different elements, particularly metals, has been of considerable interest. Of course, the simplest compounds to study this interaction are the corresponding monocyanides. However, we should first note that what are called monocyanides do not always have a M−CN arrangement. Because of the peculiar characteristics of cyanide as a ligand, with quasi-isotropic charge distribution, in many cases, monocyanides are typical examples of polytopic systems where the M^+ ion can be seen as orbiting around the CN^- moiety.[1−3] This is the case for alkaline cyanides, which are generally considered to adopt a T-shape structure.[4] On the other hand, alkaline earth elements, aluminum, gallium, and indium all are found to prefer the linear isocyanide geometry,[5−12] and therefore should be formulated as M−NC.

In recent years, there has been a renewed interest from the experimental point of view in determining the molecular structure of these monoligand compounds. In part, this interest has been motivated by the observation of different cyanides and isocyanides in the interstellar medium. So far, MgCN, MgNC, AlNC, NaCN, SiCN, and SiNC have been detected in space.[13−18] Furthermore, transition metals, such as iron, manganese, nickel, or zinc are relatively abundant in space.[19] In fact, the first compound containing a transition metal, FeO, has been tentatively identified by radioastronomy observations.[20] This suggests that other molecular species containing transition metals, and in particular cyanides or isocyanides, could be reasonable candidates for interstellar detection.

In recent years, an increasing number of cyanides and isocyanides of transition metals have been synthesized in terrestrial laboratories and subsequently studied by spectroscopic techniques. Lie and Dagdigian[21] observed FeNC by laser fluorescence excitation spectroscopy, whereas the Ziurys group[22−25] has determined precise structures for CuCN, ZnCN, NiCN, and CoCN. Very recently, Ziurys et al. characterized the pure rotational spectrum of CrCN.[26] NiCN has also been studied in separate experiments by Kingston et al.,[27] who reported its electronic and pure rotational spectra. Finally, Boldyrev et al.[28] studied the photoelectron spectra of $CuCN^-$ and $AgCN^-$.

In addition, several theoretical studies have been carried out to determine the molecular structure of individual cyanides and isocyanides of transition metals. Boldyrev et al.[28] complemented their experimental studies on $CuCN^-$ and $AgCN^-$ with ab initio studies of these anions and their neutral parent molecules. NiCN has been the subject of a preliminary theoretical study by Bauschlicher,[29] followed by a very complete ab initio study of nickel cyanide and isocyanide by Paul et al.[30] A careful study of the FeCN/FeNC system has been carried out at the theoretical level by DeYonker et al.[31] and Hirano et al.,[32] whereas the bonding in CuCN and CuNC has been addressed by Nelin et al.[33] and Dietz et al.[34]

In the present paper, we report a systematic study of first-row transition metal cyanides and isocyanides. Of course, a primary goal of the present work is to provide theoretical

* To whom correspondence should be addressed. E-mail: alargo@qf.uva.es. Fax: 34-983-423013.
[†] Universidad de Valladolid.
[‡] Academy of Sciences, Czech Republic.

10.1021/jp072434n CCC: $37.00
Published on Web 06/20/2007

predictions for these systems, because many of them have not been previously studied. In addition, a theoretical study at uniform levels of theory along the first-row transition metal series might allow a detailed knowledge of the factors governing the molecular structure and properties of these compounds. Similar systematic studies carried out previously for other related systems, such as metal dicarbides,[35,36] proved very useful in this direction.

Computational Methods

Optimized geometries for the different M(CN) systems (M = Sc−Zn) have been obtained employing two different theoretical approaches. First, density functional theory (DFT) calculations have been carried out in order to optimize the geometry. In particular, we used the B3LYP exchange-correlation functional,[37,38] which includes the Lee−Yang−Parr[39] correlation functional in conjunction with a hybrid exchange functional first proposed by Becke.[40] Second, additional geometry optimizations have been performed at the QCISD level,[41] which corresponds to quadratic configuration interaction including single and double excitations. In both cases, B3LYP and QCISD, we employed different basis sets, but we will report only those results obtained with the basis set denoted as 6-311+G(3df). This basis set includes diffuse and polarization functions and is constructed employing the triple split-valence 6-311G[42] for carbon and nitrogen atoms, and the Wachters[43] and Hay[44] basis set with the scaling factor of Ragavachari and Trucks[45] for the first-row transition metal. Harmonic vibrational calculations have been performed at the B3LYP level with the 6-311+G(3df) basis set. On the other hand, QCISD vibrational frequencies have been computed with the 6-311+G(d) basis set (at the corresponding QCISD/6-311+G(d) geometries). The computation of vibrational frequencies allows an assessment of the nature of the stationary points on the potential energy surface, as well as an estimate of the zero-point vibrational energy (ZPVE).

To refine the electronic energy, we have carried out single-point calculations on the QCISD/6-311+G(3df) geometries at the CCSD(T) level[46] (coupled-cluster single and double excitation model augmented with a noniterative treatment of triple excitations) employing the 6-311+G(3df) basis set. In all correlated calculations, we have included the valence electrons of the carbon and nitrogen atoms and the 4s and 3d electrons of the metal. The atomic states have been obtained following the rules given by Hay[44] for the occupation of the d orbitals. All these calculations were carried out with the *Gaussian-98* program package.[47]

When dealing with transition metal compounds, a matter of concern is the possible multiconfigurational nature of states under study. Therefore, in order to check the adequacy of monoconfigurational theoretical methods, we have carried out CASSCF[48,49] (complete active space multiconfiguration self-consistent field) optimizations followed by MRCI[50,51] (multireference singles and doubles configuration interaction) single-point calculations to improve the energy. In these multiconfigurational calculations, we employed the 6-311+G(d) basis set. We have considered in the active space all valence electrons, except the low-lying 2s electrons of carbon and nitrogen, distributed in 12 orbitals (including the 4s and 3d orbitals of the metal). For the MRCI calculations, all configurations with a coefficient larger than 0.01 in the CASSCF wavefunction have been taken into account. The only exception was Mn(CN), for which a threshold of 0.08 has been used because of computational limitations. The sum of the squared norms of the selected reference configuration coefficients was between 0.996 and 0.999 (except in Mn(CN), 0.934). All valence electrons of carbon and nitrogen and the 4s and 3d electrons of the metal atoms have been correlated in the MRCI calculations. The MOLPRO suite of programs[52] was employed for these calculations.

The nature of bonding for the different cyanides and isocyanides was characterized through the topological analysis of the electronic density.[53] For these calculations, we used the MORPHY program,[54] employing the QCISD/6-311+G(d) electronic density. Atomic charges were also computed with the natural bond orbital (NBO)[55] procedure. In addition, an energy decomposition analysis (EDA)[56−60] of first-row transition metal cyanides and isocyanides has been carried out, in order to obtain more detailed information about the nature of the bond in these compounds.

Results and Discussion

Molecular Structure of M(CN) Compounds. The electronic configurations, optimized geometries, and vibrational frequencies for the lowest-lying states of the different linear cyanide and isocyanide species are given in Tables 1 and 2, respectively. We have also searched for bent (C_s) states but all the optimizations finally led to linear structures. All cyanide and isocyanide isomers were found to be true minima on the respective potential energy surface. Only for the $^3\Phi$ electronic state of CoNC (see below) did we find a small imaginary frequency (33 i cm^{-1}) at the B3LYP level. A B3LYP optimization of the system in C_s symmetry leads to a minimum ($^3A''$ electronic state) that deviates only slightly from linearity (with a bond angle of 179.98°) and an energy that is identical up to the sixth decimal figure to the $C_{\infty v}$ structure. In addition, at the QCISD level, all frequencies were found to be real. Therefore, we can safely consider the $^3\Phi$ electronic state of CoNC to be linear.

All lowest-lying states for the different cyanides and isocyanides correlate with the M(ground-state) + CN($^2\Sigma^+$) asymptote. For early transition metals, Sc−Fe, the high-spin state for cyanides and isocyanides is preferred, with the only exception of Cr, because Cr(^{7}S)+CN($^2\Sigma^+$) correlates with the $^6\Sigma^+$ ground state of Cr(CN). On the other hand, for late transition metals, Co−Zn, the low-spin state is always obtained.

As discussed in the Introduction section, experimental studies have been conducted for some cyanides and isocyanides of late transition metals.[21−27] In particular, these studies have concluded that the corresponding ground states are as follows: CrCN ($^6\Sigma^+$), FeNC ($^6\Delta$); CoCN ($^3\Phi$); NiCN ($^2\Delta$); CuCN ($^1\Sigma^+$); ZnCN ($^2\Sigma^+$). We have obtained in our theoretical studies the same electronic ground states.

The CoCN system is particularly interesting, because it has not been the subject of any previous theoretical study. The experimental assignment of a $^3\Phi$ ground state is based on the identification of the three spin components that comprise this term, as well as in the analogy with other isovalent cobalt-bearing species, such as CoH, CoF, and CoCl, all having $^3\Phi$ ground states. In our explorations on the Co(CN) system, we identified two close-lying states, namely $^3\Phi$ and $^3\Delta$. Single-reference methods suggest a $^3\Delta$ ground state, although the $^3\Phi$ state lies very close in energy, namely 1.48 and 0.53 kcal mol^{-1}, at the B3LYP/6-311+G(3df) and CCSD(T)/6-311+G(3df) levels of theory, respectively. These relative energies can be considered to be smaller than the expected precision of the employed methods, and therefore what these theoretical calculations might suggest is that both states are nearly isoenergetic. However, MRCI calculations, which should be in this case more reliable given the multiconfigurational nature of the $^3\Phi$ state

TABLE 1: Electronic Configurations, Geometrical Parameters, and Harmonic Vibrational Frequencies for Linear MCN Species Obtained with the B3LYP/6-311+G(3df), QCISD/6-311+G(3df) (second line), and CASSCF/6-311+G(d) (in parentheses) Methods (QCISD vibrational frequencies have been computed with the 6-311+G(d) basis set)

		linear geometry (Å)		
linear MCN	electronic configuration	R(M−C)	R(C−N)	vibrational frequencies (cm^{-1})
ScCN ($^3\Delta$)	{core}$8\sigma^2 9\sigma^2 10\sigma^2 3\pi^4 11\sigma^1 1\delta^1$	2.225 (2.304)	1.159 (1.174)	169(π), 398(σ), 2233(σ)
		2.281	1.166	138(π), 379(σ), 2165(σ)
TiCN ($^4\Phi$)[a]	{core}$8\sigma^2 9\sigma^2 10\sigma^2 3\pi^4 1\delta^1 4\pi^1 11\sigma^1$	2.122 (2.225)	1.160 (1.177)	187(π),198(π),410(s), 2220(σ)
		2.175	1.166	163(π), 395(σ), 2132(σ)
VCN ($^5\Delta$)	{core}$8\sigma^2 9\sigma^2 10\sigma^2 3\pi^4 1\delta^1 4\pi^2 11\sigma^1$	2.046 (2.170)	1.160 (1.177)	219(π), 418(σ), 2212(σ)
		2.089	1.166	186(π), 413(σ), 2118(σ)
CrCN ($^6\Sigma^+$)	{core}$8\sigma^2 9\sigma^2 10\sigma^2 3\pi^4 1\delta^2 4\pi^2 11\sigma^1$	2.021 (2.157)	1.159 (1.178)	223(π), 418(σ), 2224(σ)
		2.061	1.166	189(π), 401(σ), 2141(σ)
MnCN ($^7\Sigma^+$)	{core}$8\sigma^2 9\sigma^2 10\sigma^2 3\pi^4 1\delta^2 4\pi^2 11\sigma^1 12\sigma^1$	2.098 (2.169)	1.159 (1.177)	157(π), 388(σ), 2232(σ)
		2.117	1.164	153(π), 387(σ), 2177(σ)
FeCN ($^6\Delta$)	{core}$8\sigma^2 9\sigma^2 3\pi^4 10\sigma^2 1\delta^3 11\sigma^1 4\pi^2 12\sigma^1$	2.042 (2.113)	1.158 (1.176)	169(π), 408(σ), 2233(σ)
		2.057	1.163	169(π), 410(σ), 2181(σ)
CoCN ($^3\Phi$)[a]	{core}$8\sigma^2 9\sigma^2 3\pi^4 10\sigma^2 11\sigma^2 4\pi^3 1\delta^3$	1.898 (1.939)	1.158 (1.177)	252(π), 265(π), 446(σ), 2234(σ)
		1.931	1.164	142(π), 261(π), 443(σ), 2120(σ)
NiCN ($^2\Delta$)	{core}$8\sigma^2 9\sigma^2 3\delta^4 10\sigma^2 4\pi^4 11\sigma^2 1\delta^3$	1.848 (1.970)	1.157 (1.175)	255(π), 476(σ), 2249(σ)
		1.879	1.164	224(π), 450(σ), 2215(σ)
CuCN ($^1\Sigma^+$)	{core}$8\sigma^2 9\sigma^2 3\delta^4 10\sigma^2 1\delta^4 4\pi^4 11\sigma^2$	1.849 (1.962)	1.157 (1.174)	251(π), 463(σ), 2257(σ)
		1.868	1.163	235(π), 461(σ), 2216(σ)
ZnCN ($^2\Sigma^+$)	{core}$8\sigma^2 9\sigma^2 1\delta^4 3\pi^4 10\sigma^2 4\pi^4 11\sigma^2 12\sigma^1$	1.977 (2.000)	1.156 (1.177)	181(π), 397(σ), 2263(σ)
		1.963	1.163	197(π), 413(σ), 2126(σ)

[a] Note that nondegenerate π vibrational frequencies corresponding to the two Renner−Teller components are obtained in this case.

TABLE 2: Electronic Configurations, Geometrical Parameters, and Harmonic Vibrational Frequencies for Linear MNC Species Obtained with the B3LYP/6-311+G(3df), QCISD/6-311+G(3df) (second line) and CASSCF/6-311+G(d) (in parentheses) Methods (QCISD vibrational frequencies have been computed with the 6-311+G(d) basis set)

		linear geometry (Å)		
linear MNC	electronic configuration	R(M−N)	R(C−N)	vibrational frequencies (cm^{-1})
ScNC ($^3\Delta$)	{core}$8\sigma^2 9\sigma^2 10\sigma^2 3\pi^4 11\sigma^1 1\delta^1$	2.067 (2.138)	1.176 (1.187)	115(π), 467(σ), 2114(σ)
		2.123	1.180	95(π), 437(σ), 2086(σ)
TiNC ($^4\Phi$)[a]	{core}$8\sigma^2 9\sigma^2 10s^2 3\pi^4 1\delta^1 4\pi^1 11\sigma^1$	1.997 ((2.085)	1.176 (1.189)	146(π),148(π),476(σ), 2105(σ)
		2.044	1.180	122(π), 450(σ), 2086(σ)
VNC ($^5\Delta$)	{core}$8\sigma^2 9\sigma^2 10\sigma^2 3\pi^4 1\delta^1 4\pi^2 11\sigma^1$	1.952 (2.047)	1.175 (1.188)	165(π), 475(σ), 2109(σ)
		1.983	1.179	139(π), 465(σ), 2091(σ)
CrNC ($^6\Sigma^+$)	{core}$8\sigma^2 9\sigma^2 10\sigma^2 3\pi^4 1\delta^2 4\pi^2 11\sigma^1$	1.928 (1.989)	1.174 (1.187)	161(π), 468(σ), 2121(σ)
		1.941	1.178	135(π), 466(σ), 2099(σ)
MnNC ($^7\Sigma^+$)	{core}$8\sigma^2 9\sigma^2 10\sigma^2 3\pi^4 1\delta^2 4\pi^2 11\sigma^1 12\sigma^1$	1.980 (2.050)	1.175 (1.189)	99(π), 448(σ), 2113(σ)
		1.999	1.179	91(π), 437(σ), 2093(σ)
FeNC ($^6\Delta$)	{core}$8\sigma^2 9\sigma^2 3\pi^4 10\sigma^2 1\delta^3 11\sigma^1 4\pi^2 12\sigma^1$	1.923 (1.994)	1.177 (1.189)	110(π), 471(σ), 2106(σ)
		1.938	1.179	107(π), 466(σ), 2093(σ)
CoNC ($^3\Phi$)[a]	{core}$8\sigma^2 9\sigma^2 3\pi^4 10\sigma^2 11s^2 4\pi^3 1\delta^3$	1.841 (1.847)	1.173 (1.188)	33 i(π), 168(π), 482(σ), 2129(σ)
		1.862	1.177	108(π), 142(π), 475(σ), 2108(σ)
NiNC ($^2\Sigma^+$)	{core}$8\sigma^2 9\sigma^2 3\pi^4 10\sigma^2 4\pi^4 1\delta^4 11\sigma^1$	1.824 (1.930)	1.171 (1.186)	167(π), 491(σ), 2148(σ)
		1.837	1.176	158(π), 484(σ), 2118(σ)
CuNC ($^1\Sigma^+$)	{core}$8\sigma^2 9\sigma^2 3\pi^4 10\sigma^2 1\delta^4 4\pi^4 11\sigma^2$	1.811 (1.888)	1.171 (1.186)	152(π), 490(σ), 2153(σ)
		1.818	1.176	141(π), 497(σ), 2118(σ)
ZnNC ($^2\Sigma^+$)	{core}$8\sigma^2 9\sigma^2 1\delta^4 3\pi^4 10\sigma^2 4\pi^4 11\sigma^2 12\sigma^1$	1.891 (1.914)	1.173 (1.190)	103(π), 444(σ), 2141(σ)
		1.873	1.178	109(π), 460(σ), 2107(σ)

[a] Note that nondegenerate π vibrational frequencies corresponding to the two Renner−Teller components are obtained in this case.

(vide infra), seem to favor a $^3\Phi$ ground state because the $^3\Delta$ is found to lie about 3.55 kcal mol^{-1} higher in energy. For the isocyanide isomer, CoNC, the situation is quite similar. Single-reference methods place the $^3\Delta$ state slightly below the $^3\Phi$ state, but again, MRCI calculations show that the $^3\Phi$ should be the ground state (4.6 kcal mol^{-1} below the $^3\Delta$). Therefore, in agreement with the experiment, we have adopted the $^3\Phi$ state for the Co(CN) system.

Another interesting case is NiCN. Our theoretical calculations agree with the experimental observation of a $^2\Delta$ ground state, but we have found that the $^2\Sigma^+$ state lies very close in energy (within less than 1 kcal mol^{-1} at both B3LYP/6-311+G(3df) and CCSD(T)/6-311+G(3df) levels). This result agrees with the predictions of Paul et al.,[30] who also find the $^2\Delta$ state slightly lower in energy than the $^2\Sigma^+$ state. For the isocyanide isomer, NiNC, we obtain the $^2\Sigma^+$ state lying below the corresponding $^2\Delta$ by about 13.9 kcal mol^{-1} at the CCSD(T) level of theory, a result that is confirmed by the MRCI calculations (the $^2\Delta$ state lies about 13.2 kcal mol^{-1} above the $^2\Sigma^+$ state at this level of theory).

We shall briefly comment the geometrical parameters shown in Tables 1 and 2. First, the agreement between the B3LYP and QCISD geometries is rather good, as well as the vibrational frequencies. The geometrical parameters are also in reasonable agreement with the available experimental measures from rotational spectroscopy.[22−26] Ziurys et al.[22−26] obtained the following values for M−C distances in cyanides from their pure rotational spectroscopy experiments: 2.019 Å (CrCN); 1.8827 Å (CoCN); 1.8263 Å (NiCN); 1.8296 Å (CuCN); 1.9496 Å (ZnCN). Incidentally, it can be observed that the B3LYP optimized M−C distances are generally slightly closer to the experimental values. The agreement is slightly poorer for the

C−N distances. In the same rotational experiments, Ziurys et al.[22−26] obtained the following C−N distances: 1.148 Å (CrCN); 1.1313 Å (CoCN); 1.152 Å (NiCN); 1.1621 Å (CuCN); 1.1417 Å (ZnCN). Nevertheless, it should be mentioned that, as discussed by Ziurys and co-workers[22−26] and Paul et al.,[30] the flat bending potential in cyanides may lead to the prediction of somewhat short C−N distances from the experimental data. In the case of the only first-row transition metal isocyanide observed experimentally, FeNC, the estimated geometrical parameters from the laser fluorescence excitation spectroscopy by Lie and Dagdigian[21] are 2.01 Å (Fe−N) and 1.03 Å (C−N). Even though the value for the C−N distance is clearly very low (much shorter than any known C−N bond distance), probably as a consequence of the uncertainties involved in the determination of the rotational constant from the laser excitation fluorescence spectra, it must be recognized that for FeNC, the B3LYP and QCISD geometrical parameters are in relatively poor agreement with the experimental values. Nevertheless, our results for this system are very similar to other theoretical values obtained with high-level methods, such as CCSD or MRCISD+Q, carried out by DeYonker et al.[31]

To assess the possible multireference character of these molecules, we have also carried out CASSCF geometry optimizations. The resulting geometrical parameters are also collected in Table 1 and complete the following trend in the M−C/N bond distances: B3LYP < QCISD < CASSCF. We have found that, with the exception of Ti(CN) ($^3\Phi$), Co(CN) ($^3\Phi$), and NiCN ($^2\Delta$), the ground states of the first-row transition metal cyanides are clearly dominated by single configurations. Thus, single-reference correlated methods should be reliable for the study of these species.

The general trend in M−C distances (cyanides) and in M−N distances (isocyanides) along the series is a shortening from Sc to Cr, a slight lengthening for Mn, and finally a smooth shortening again from Fe to Cu. This trend essentially follows the decrase in the atomic radii of the metal from the left to the right in the first transition row. The C−N distances are very close for all cyanides and slightly shorter than for cyanogen. For CN, the B3LYP/6-311+G(3df) method provides 1.162 Å, whereas at the QCISD/6-311+G(3df) level, a distance of 1.175 Å is found. On the other hand, the C−N distances in isocyanides are generally slightly longer than those in cyanogen. Therefore, it seems from the geometrical parameters that bonding to the CN moiety of a transition metal through the carbon atom slightly reinforces the C−N bond, whereas it is slightly weakened if the bonding takes place through the nitrogen atom.

This effect is also reflected in the vibrational frequencies. Whereas the C−N stretching frequency for the different cyanides is slightly larger than the value found in cyanogen (2151 and 2149 cm^{-1}, respectively, at the B3LYP and QCISD levels), for the isocyanides, the C−N stretching frequency is generally smaller. Therefore, we may conclude that the C−N stretching is blue-shifted for cyanides and red-shifted for isocyanides, as expected. We should stress that the tabulated values in Tables 1 and 2 are unscaled harmonic vibrational frequencies. To predict these values more precisely, we should employ scale factors. For example, the experimental vibrational frequency[61] for the cyanogen radical is 2068.59 cm^{-1}, and therefore a possible scale factor for the C−N stretching for both B3LYP and QCISD levels is 0.962. The available experimental[28] value for the M−C stretching, the Cu−C stretching frequency in CuCN of 480 cm^{-1}, compares rather well with the predicted theoretical values in Table 1 (463 and 461 cm^{-1}, respectively, at the B3LYP and QCISD levels). In the case of FeNC, the estimated value for the Fe−N stretching from experimental measures[21] is 464 cm^{-1}, also in good agreement with the B3LYP (471 cm^{-1}) and QCISD (466 cm^{-1}) values. It is also worth mentioning that the most intense signal in the theoretically predicted IR spectra at both levels, B3LYP and QCISD, corresponds to the M−C stretching for the cyanides (the C−N stretching has significant intensities, but sensibly lower than M−C). In the case of isocyanides, even though the M−N stretching also has a noticeable intensity, the most intense signal comes from the C−N stretching. For both cyanides and isocyanides, the bending mode is predicted to be almost inactive in the infrared in most cases. The infrared intensities and dipole moments, which might be useful for experimental searches, are given as Supporting Information (Tables S1 and S2).

TABLE 3: Relative Energies ($E_{MNC}-E_{MCN}$; kcal mol^{-1}) for Different First-Row Transition Metal Cyanides and Isocyanides at Different Levels of Theory with the 6-311+G(3df) Basis Set and Including ZPVE Corrections; in the Cases of QCISD, CCSD(T), and MRCI Calculations, QCISD/6-311+G(d) ZPVE Values Have Been Employed

	level			
	B3LYP	QCISD	CCSD(T)	MRCI
Sc(CN) ($^3\Delta$)	−5.50	−4.99	−4.54	−3.77
Ti(CN) ($^4\Phi$)	−2.65	−2.92	−2.53	−1.40
V(CN) ($^5\Delta$)	0.94	−0.32	−0.03	0.48
Cr(CN) ($^6\Sigma^+$)	2.42	3.63	4.90	9.86
Mn(CN) ($^7\Sigma^+$)	−1.03	−0.65	−0.12	−1.38
Fe(CN) ($^6\Delta$)	−1.30	−0.79	−0.25	1.71
Co(CN) ($^3\Phi$)	7.26	6.22	14.71	8.40
Ni(CN) ($^2\Sigma^+-{}^2\Delta$)	9.24	7.80	8.72	10.05[a]
Cu(CN) ($^1\Sigma^+$)	10.74	8.65	10.18	10.96
Zn(CN) ($^2\Sigma^+$)	4.81	4.46	5.11	6.80

[a] For technical reasons, we have used the natural orbitals from a singles and doubles configuration interaction (CISD) wavefunction in the MRCI procedure.

Cyanide−Isocyanide Competition and Isomerization Barriers. One of the most interesting questions concerning M(CN) systems is the competition between cyanide and isocyanide isomers. We have already mentioned in the Introduction that experimental observations have been made for CrCN, CoCN, NiCN, CuCN, and ZnCN (from rotational spectroscopy[22−26]), and for FeNC (through fluorescence excitation spectroscopy[21]). Therefore, experimental work on M(CN) systems suggest that late transition metals prefer a cyanide arrangement. This trend seems to be reversed for iron, because the Fe(CN) system shows a preference for the isocyanide form. However, the detailed theoretical study by DeYonker et al.[31] found the iron cyanide and isocyanide forms to be nearly isoenergetic, with a slight preference for the isocyanide isomer, which is predicted to lie just 0.6 kcal mol^{-1} below the cyanide isomer. Whether this inversion in the trend should imply that early transition metals should prefer cyanide isomers over isocyanide ones is not known at present time.

To provide information that could shed light into this question, the relative energies for the cyanide and isocyanide isomers of first-row transition metals are given in Table 3. A remarkably good agreement is observed for the results provided by different theoretical methods. B3LYP, QCISD, and CCSD(T) methods agree in all cases not only qualitatively but also from the quantitative point of view. There is only one discrepancy in the predicted lowest-lying isomer. Whereas both CCSD(T) and QCISD predict that the isocyanide isomer should be the global minimum for V(CN), the B3LYP methods points to the cyanide form as the most stable one in this case. However, it should be noticed that the difference in relative energy between CCSD-

(T) and B3LYP is less than 1 kcal mol^{-1}, and in fact, both species seem to be almost isoenergetic at the most reliable level, namely CCSD(T).

The results shown in Table 3 agree with the experimental observation of a preference for the cyanide isomer for Co−Zn, as well as with the experimentally observed isocyanide isomer for Fe(CN). They also agree with previous available theoretical studies. As already mentioned before, DeYonker et al.[31] predict FeNC to lie 0.6 kcal mol^{-1} below FeCN; Paul et al.[30] obtained for the Ni(CN) system that the cyanide isomer lies lower in energy than the isocyanide isomer by 12.2 kcal mol^{-1}; finally, Dietz et al.[34] found CuCN to lie 10.0 kcal mol^{-1} below CuNC.

The main conclusion from the results shown in Table 3 is that early transition metals do, in fact, show a preference for the isocyanide isomers. This seems to be strictly true for Sc and Ti. In the cases of V(CN), Mn(CN), and Fe(CN), the theoretical results suggest that the isocyanide isomer should be preferred, but both isomers are found to be nearly isoenergetic, especially at the most reliable level of theory CCSD(T), and it is difficult to establish a definitive conclusion. For Cr(CN), all theoretical methods agree in that the cyanide is preferred over the isocyanide isomer, in agreement with the experimental evidence. We would like to draw the reader's attention to the relationship that seems to exist between the conformational preference and the metal−ligand bond distance: those systems with the longest bond distance, Sc(CN) and Ti(CN), are isocyanides, whereas those with the shortest one, from Co(CN) to Zn(CN), are cyanides. From V(CN) to Fe(CN), we observe intermediate bond distances and the isomers have similar energies. An analysis of the bonding and its relation to the conformational preference will be the topic of the following section.

We have also analyzed the variation of the energy of the M(CN) systems with the ∠MCN φ angle, starting from $\varphi = 0°$ (corresponding to the MNC isomer) up to $\varphi = 180°$ (MCN isomer), and the results are shown in Figure 1. The graphs have been obtained optimizing at the B3LYP/6-311+G(d) level the geometry for fixed φ angles, followed by single-point energy calculations at the CCSD(T)/6-311+G(d) level. The only exception is the Co(CN) system, in which the B3LYP energies are represented because of problems of convergence in the coupled cluster method for some points.

Most of the systems behave in the expected way, passing through a maximum (an approximation to the transition state for the isomerization process) as one moves from the isocyanide to the cyanide isomer. However, there are two systems that appear to behave in a different form than the rest, namely Co(CN) and Ni(CN). For Ni, a shoulder in the curve is observed, whereas for Co, even two different transition states are found, consequently leading to an apparent cyclic (T-shape) minimum in between. This anomalous behavior of the Co(CN) system is a consequence of the avoided crossing of the ^{3}A″ states resulting from the $^3\Delta$ and $^3\Phi$ states. The two transition states correspond to the processes CoNC($^3\Delta$) → CoCN($^3\Delta$) and CoNC($^3\Phi$) → CoCN($^3\Phi$), respectively. Because in this case both transition states have rather different bond angles, they are located in separate regions of the potential energy surface, and therefore, when one follows the rearrangement process (C_s symmetry), two transition states and an apparent minimum can be located. In the case of the Ni(CN), a similar behavior is observed. Both $^2\Delta$ and $^2\Sigma^+$ states lead to ^{2}A′ in C_s symmetry. However, for Ni(CN), both transition states are geometrically closer and only a shoulder appears in the curve.

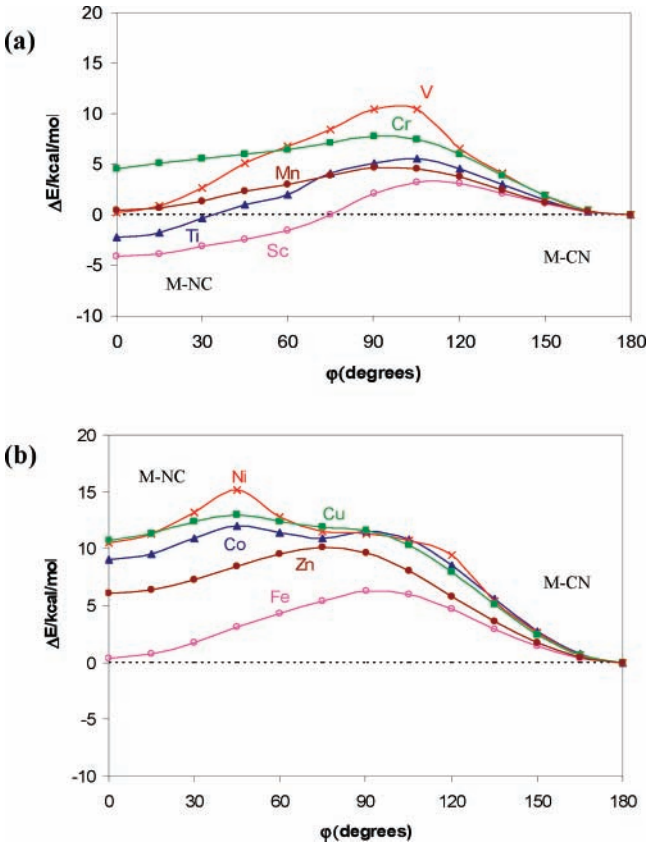

Figure 1. Variation of the total energy (in kcal/mol, relative to the MCN isomer), computed at the CCSD(T)/6-311+G(d)//B3LYP/6-311+G(d) level, for the different M(CN) compounds with the bond angle ($\varphi = 0°$ corresponds to the isocyanide isomer, whereas $\varphi = 180°$ corresponds to the cyanide one). In the case of Co(CN), the B3LYP/6-311+G(d) values are represented. (a) Results of early transition metals (Sc−Mn), and (b) results for late transition metals (Fe−Zn).

It can be seen in Figure 1 that in general, early transition metals show a less pronounced variation of the energy with the bond angle than late transition metals. In that sense, apparently the early transition metal cyanides approach a polytopic behavior,[1] typical of ionic compounds. Similar patterns are found within the two series. For example, the Sc, Ti, and V curves are almost parallel with increasing relative energies. For Cr and Mn, the trend is reversed. For late transition metals, we observe increasing relative energies for the series Fe, Co, and Ni, whereas for Cu and Zn, relative energies again decrease.

We have optimized the transition states for the isocyanide → cyanide conversion. The geometrical parameters for the different transition states are provided as Supporting Information (Table S3), whereas the isomerization barriers (relative in all cases to the MNC isomer) are given in Table 4. It is worth noting that the B3LYP method seems to perform rather well for predicting isomerization barriers, because it provides results very similar to those obtained at the CCSD(T) level, in most cases within 2 kcal mol^{-1}. The only exception is Cr(CN), where a discrepancy of more than 4 kcal mol^{-1} is observed.

Our computed MNC→MCN barriers are close to the previously estimated values, when available. To the best of our knowledge, the isomerization barrier has been computed for the Cu(CN) and Fe(CN) systems. Boldyrev et al.[28] have studied the CuNC → CuCN barrier, obtaining values of 4.4 and 1.8 kcal mol^{-1} at the B3LYP/6-311+G(d) and MP2/6-311+G(d) levels, respectively. As can be seen in Table 5, we predict a barrier of 3.73 kcal mol^{-1} at the B3LYP/6-311+G(3df) level and 2.86 kcal mol^{-1} at the CCSD(T)/6-311+G(3df). In the case

TABLE 4: Barrier for the MNC−MCN Isomerization (kcal mol^{-1}) for Different First-Row Transition Metal Cyanides at Different Levels of Theory with the 6-311+G(3df) Basis Set and Including ZPVE Corrections; in the Cases of QCISD and CCSD(T) Calculations, QCISD/6-311+G(d) ZPVE Values Have Been Employed and in All Cases, the Barrier Is Computed Relative to the MNC Isomer

	level		
	B3LYP	QCISD	CCSD(T)
ScCN ($^3\Delta$)	9.53	8.37	7.78
TiCN ($^4\Phi$)	9.15	8.63	8.07
VCN ($^5\Delta$)	11.21	10.79	10.51
CrCN ($^6\Sigma^+$)	7.94	4.31	3.13
MnCN($^7\Sigma^+$)	5.92	5.71	4.96
FeNC ($^6\Delta$)	7.62	7.43	6.62
CoCN($^3\Phi$)	1.90	5.85	5.80
NiCN ($^2\Delta\rightarrow{}^2\Sigma^+$)	4.32	5.25	4.95
CuCN ($^1\Sigma^+$)	3.73	3.73	2.86
ZnCN ($^2\Sigma^+$)	5.28	5.38	4.53

TABLE 5: Dissociation Energies (kcal mol^{-1}) of Different First-Row Transition Metal Cyanides and Isocyanides at the B3LYP and CCSD(T) Levels of Theory, Including ZPVE Corrections, with the 6-311+G(3df) Basis Set; in the Case of CCSD(T) Calculations, QCISD/6-311+G(d) ZPVE Values Have Been Employed

	MCN		MNC	
M	B3LYP	CCSD(T)	B3LYP	CCSD(T)
Sc	103.41	96.42	108.91	100.95
Ti	105.83	96.23	108.47	98.76
V	110.63	99.28	109.69	99.30
Cr	95.67	94.61	93.24	89.72
Mn	80.25	81.19	81.28	81.48
Fe	80.92	80.97	82.22	81.22
Co	97.87	88.15	85.76	73.44
Ni	107.78	101.71	98.55	92.99
Cu	95.15	97.08	84.41	86.89
Zn	52.57	54.99	47.76	49.87

of the FeNC → FeCN barrier, our computed value of 6.62 kcal mol^{-1} at the CCSD(T) level coincides with that obtained by DeYonker et al.[31] using MRCISD+Q/cc-pVQZ energies at CASSCF geometries, namely 6.5 kcal mol^{-1}.

With very few exceptions (perhaps the most noticeable being Mn(CN)), the geometrical parameters of the transition states at the B3LYP and QCISD levels are quite similar (see Table S3 in the Supporting Information). As a general trend, the ∠MCN angle for the transition state decreases along the transition metal series, although for the last member of the series (the Zn(CN) system), the angle increases significantly again. This essentially reflects a progressive preference for the cyanide form as one moves from the left to right side of the transition metal series. A similar trend is observed for the isomerization barrier, with larger barriers for early transition metals than for late ones. Probably the most noticeable exception is the rather low barrier found for the Cr(CN) system, which is only 3.13 kcal mol^{-1} at the CCSD(T) level. In general, even for early transition metals, moderate or even low barriers are encountered. This is probably due to a low degree of covalency in the metal−cyanide bonds. It has been generally suggested[10,27] that an increasing degree of covalency enhances the height of the barrier. The relatively small barriers observed for M(CN) systems suggest a low degree of covalency.

We have also computed the dissociation energies for both cyanides and isocyanides, that is, the energy associated to the process M(CN) → M + CN. The results at both B3LYP and CCSD(T) levels, including ZPVE corrections, are shown in Table 5. It is readily seen that in some cases (Cr, Mn, Fe, Cu, Zn), the agreement between both levels of theory is good. However, for the rest of species, the dissociation energies for both cyanides and isocyanides differ considerably when computed at B3LYP and CCSD(T) levels. In these cases, the difference between both sets of values is within 7−12 kcal mol^{-1}. However, it is generally observed that the relative ordering in stability agrees for both levels of theory to a large extent. Therefore, it seems that even though B3LYP dissociation energies might not be accurate enough for quantitative purposes, they qualitatively reflect the relative stability of cyanides and isocyanides along the first transition series.

The general trend observed for dissociation energies, in both cyanides and isocyanides, is that the largest values are found for the early transition metals (Sc, Ti, V). Dissociation energies then decrease, taking smaller values for Mn, Fe, and Co, and then a second increment is observed up to Ni. In fact, the largest dissociation energy is obtained for NiCN (CCSD(T) level). As one moves toward the last member of the series, Zn, dissociation energies again decrease. The smallest values, nearly half the dissociation energy found for Ni(CN), is obtained for Zn(CN). In general, both cyanides and isocyanides are quite stable toward fragmentation into M + CN, showing in most cases dissociation energies within the range 80−100 kcal/mol. Only Zn(CN) species have smaller values.

It is interesting to point out that all experimentally observed cyanides/isocyanides correspond to late transition metals (Fe−Zn),[21−28] including ZnCN, which according to our results is not particularly stable (dissociation energy around 55 kcal/mol). Therefore, it is expected that cyanides/isocyanides of early transition metals (Sc−Cr), which exhibit the largest dissociation energies, could also be reasonable experimental targets.

Analysis of the Bonding. Of course, an important challenge from the theoretical point of view is to provide an interpretation to the preference for cyanide or isocyanide species. We have applied different techniques in order to provide some insight into this question.

To characterize the type of interaction between the transition metal and the carbon/nitrogen atoms, we have employed the topological analysis of the electronic charge density.[53] Even though different authors have illustrated some of its possible limitations,[62−66] and therefore some caution should be exercised when evaluating the results from this kind of analysis, the topological analysis of the charge density may provide useful information.

Critical points in the one-electron density $\rho(r)$ computed at the QCISD/6-311+G(d) level were identified. Of course, for linear species, only bond critical points[53] (corresponding to a minimum value of ρ(r) along the line linking the nuclei and a maximum along the interatomic surfaces) are relevant. Only the most important properties of bond critical points, namely the electronic density ρ(r) at the critical point, the Laplacian of the charge density $\nabla^2\rho$(r), and the total energy density H(r), obtained with the QCISD/6-311+G(d) electronic density, are reported in Table 6.

The values of the charge density and its Laplacian at the bond critical point may inform us about the chemical nature of the bonding. There are basically two limiting types of atomic interactions, shared and closed-shell interactions.[53] However, a wide variety of intermediate interactions lying between these two extreme cases can be found.[67] A full account of the characteristics of the different interactions can be found in detail in the original references by Bader.[53,67] We shall just recall that shared interactions are in general characterized by large electronic densities and negative values of the Laplacian,[53] and are characteristic of covalent compounds. On the other hand,

TABLE 6: Summary of Critical Point Data for the MCN and MNC Isomers, Using the QCISD/6-311+G(d) Electronic Density

isomer	type		Sc	Ti	V	Cr	Mn	Fe	Co	Ni	Cu	Zn
MCN	M−C bond	ρ(r)	0.0565	0.0684	0.0813	0.0864	0.0754	0.0838	0.1091	0.1184	0.1183	0.0950
		$\nabla^2\rho$(r)	0.1752	0.2408	0.3000	0.2640	0.2356	0.2643	0.3528	0.4131	0.4429	0.3527
		−H(r)	0.0498	0.0724	0.0949	0.0911	0.0793	0.0880	0.1175	0.1311	0.1326	0.1000
	C−N bond	ρ(r)	0.4528	0.4523	0.4512	0.4511	0.4531	0.4532	0.4504	0.4509	0.4503	0.4500
		$\nabla^2\rho$(r)	−0.1019	−0.1045	−0.1113	−0.0989	−0.0743	−0.0625	−0.0644	−0.0490	−0.0127	−0.0092
		−H(r)	0.7677	0.7661	0.7619	0.7658	0.7768	0.7802	0.7740	0.7805	0.7883	0.7882
MNC	M−N bond	ρ(r)	0.0696	0.0802	0.0895	0.0996	0.0867	0.0971	0.1172	0.1145	0.1228	0.1050
		$\nabla^2\rho$(r)	0.3174	0.4151	0.5109	0.5150	0.4343	0.5107	0.6598	0.7563	0.7796	0.6528
		−H(r)	0.0843	0.1130	0.1407	0.1472	0.1241	0.1423	0.1801	0.1976	0.1998	0.1598
	N−C bond	ρ(r)	0.4357	0.4337	0.4392	0.4316	0.4329	0.4309	0.4277	0.4257	0.4239	0.4242
		$\nabla^2\rho$(r)	−0.3148	−0.2689	−0.1818	−0.1718	−0.2471	−0.2321	−0.1179	−0.0395	−0.0511	−0.0945
		−H(r)	0.6675	0.6735	0.7086	0.6914	0.6765	0.6748	0.6941	0.7077	0.7004	0.6910

closed-shell interactions correspond to relatively low $\rho(r)$ and positive values of $\nabla^2\rho(r)$,[53] a situation which is usually found for ionic and van der Waals compounds. We should also mention that the total energy density, $H(r)$, which is the sum of the potential and kinetic energy density at a critical point, might be useful in order to characterize the covalency degree of a bond.[68] If $H(r) < 0$, the system is stabilized by accumulation of electronic charge in the internuclear region, showing the characteristics of a covalent interaction.[68] On the other hand, positive values of $H(r)$ imply that accumulation of electronic charge would lead to a destabilization of the system, a typical feature of van der Waals and ionic bonding systems.

It is readily seen in Table 6 that the nature of the M−C/N and C−N bonds is rather different. Of course, the C−N bonds exhibit characteristics of typical covalent bonds, whereas the M−C/N bonds have small densities and positive values of $\nabla^2\rho(r)$, typical of ionic compounds. Nevertheless, the negative values of H(r) found for M−C/N bonds suggest a certain degree of covalency, and therefore, these bonds might be classified as intermediate interactions.

It is interesting to note that the critical point data for C−N bonds reflect the general trend pointed out in the preceding discussion of the molecular structure of M(CN) compounds. The values of the electronic density obtained for C−N bond critical points are always slightly larger for cyanides than for the corresponding isocyanides, a trend that is also followed by the absolute value of the total energy density. These observations probably reflect the strengthening/weakening of the C−N bond upon formation of the cyanides/isocyanides.

Concerning the M−C/N bonds, there are two basic features that should be pointed out. First, it is always observed that the M−C bonds have slightly lower $\rho(r)$ and absolute $H(r)$ values than their M−N counterparts, suggesting that M−C bonds in cyanides should be considered to have a slightly larger ionic (less covalent) character than the M−N bonds in the corresponding isocyanides. Second, both types of bonds, M−C and M−N, exhibit the same trend along the transition series: early transition metals have lower $\rho(r)$ and less negative $H(r)$ values than late transition metals. In fact, these properties vary nearly monotonically along the series. The consequence is that M−C/N bonds for early transition metals have a higher ionic character (electronic density lower than 0.1 au; less negative values of $H(r)$) than those for late transition metals.

To give more insight into the bonding in transition metal cyanides and isocyanides, we have applied an energy decomposition analysis (EDA).[56−60] Information and technical details about this method can be found in different sources.[56−60] We will just briefly comment on the significance of the main concepts employed in this analysis. In the EDA procedure, the total interaction energy between two fragments is partitioned into three components: (i) ΔE_{elstat} is the electrostatic interaction energy between the fragments, calculated with a frozen electron distribution in the geometry of the compound; (ii) ΔE_{pauli} gives the repulsive term arising from exchange repulsion; (iii) ΔE_{orb} is the stabilization due to orbital interactions, a term that can be separated into the contributions arising from the different symmetries within the point group of the molecule. The sum of these three terms gives the total interaction energy, ΔE_{int}

$$\Delta E_{\text{int}} = \Delta E_{\text{elstat}} + \Delta E_{\text{pauli}} + \Delta E_{\text{orb}} \quad (1)$$

Finally, the total bond energy is obtained taking into account the preparation energy, E_{prep}, that is, the energy necessary to promote both fragments from their equilibrium geometry and electronic ground state to the geometry and electronic state in the molecule.

We have carried out the EDA study with the BP86 functional[69,70] employing a STO triple-zeta basis set, augmented by one set of d and f polarization functions on carbon and nitrogen and one set of p (difuse) and f-type (polarization) functions on the metal.[71] The $1s^2$ core electrons of C and N and the $1s^22s^22p^6$ core electrons of the metal atoms were treated by the frozen core aproximation.[72] The EDA study has been carried out using geometries optimized at the same level of theory.

When carrying out EDA studies, one must previously define the fragments in which the system is partitioned. In our case, metal cyanides and isocyanides, we have two different possibilities. One could consider that the system is formed from M + CN, taking the neutral species as the bonding partners. Alternatively, the charged fragments, $M^+ + CN^-$, can be considered as the bonding partners. These two options correspond to homolytic and heterolytic bond breaking, respectively. Of course, in the gas phase, the dissociation of the molecule should render the homolytic fragments. In fact, we have previously discussed the stability of the transition metal cyanides and isocyanides in terms of their dissociation energies for the homolytic process. Nevertheless, there are arguments for considering the charged species as bonding partners.

First, the net atomic charges for these systems may give us some clues. In Table 7, the atomic charges obtained from a NBO analysis at the QCISD/6-311+G(3df) level are shown. In all cases, it can be observed that the partial atomic charge at the metal is within the range 0.75−0.92, strongly suggesting that a net transfer of nearly one electron from the metal to the CN moiety takes place for all cyanides and isocyanides. Even though a reasoning based on the net charges should be taken with caution, these results are compatible with the option of considering $M^+ + CN^-$ as bonding partners. We note by passing some clear trends in the atomic charges shown in Table 7. When comparing cyanides with isocyanides for the same metal, the largest positive charge at the metal is always observed for the isocyanide, where the metal is bonded to the nitrogen atom.

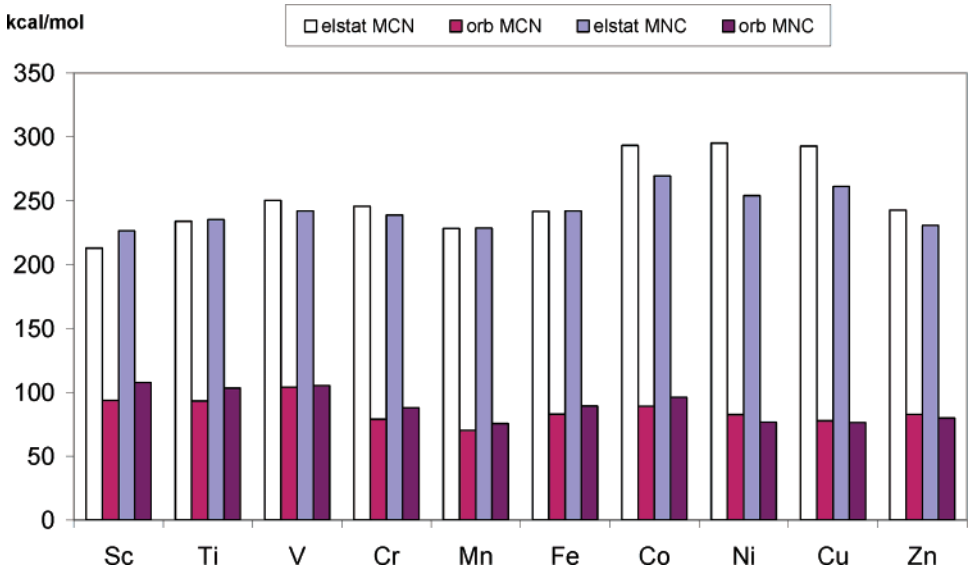

Figure 2. Electrostatic and orbital contributions (kcal mol^{-1}) from the energy decomposition analysis at the BP86/TZ2P+ level of M−CN and M−NC (M = Sc−Zn).

TABLE 7: NBO Atomic Charges and Populations of the Metal dπ Orbitals at the QCISD/6-311+G(3df) Level.

isomer	atomic charge	Sc	Ti	V	Cr	Mn	Fe	Co	Ni	Cu	Zn
MCN	Q(M)	0.884	0.842	0.785	0.780	0.897	0.869	0.752	0.752	0.757	0.826
	Q(C)	−0.471	−0.428	−0.363	−0.327	−0.428	−0.498	−0.328	−0.315	−0.324	−0.451
	Q(N)	−0.413	−0.414	−0.421	−0.454	−0.392	−0.399	−0.424	−0.437	−0.433	−0.375
	d(M)	0.012	1.111	1.970	1.974	1.996	2.004	2.970	3.944	3.959	3.980
MNC	Q(M)	0.925	0.898	0.866	0.827	0.900	0.949	0.848	0.875	0.871	0.915
	Q(N)	−1.106	−1.074	−1.027	−0.965	−1.091	−1.135	−1.006	−0.992	−1.007	−1.120
	Q(C)	0.180	0.176	0.161	0.138	0.191	0.186	0.158	0.117	0.135	0.205
	d(M)	0.024	1.050	1.977	1.985	2.003	2.016	2.995	3.953	3.963	3.981

This makes sense because of the higher electronegativity of nitrogen compared to carbon. It is also observed that for the cyanides the C and N atoms bear a negative charge of approximately the same magnitude in all cases. On the other hand, all isocyanides exhibit a negative charge at nitrogen of nearly 1 au and a small, but non-negligible (0.11−021 a.u.), positive charge at the carbon atom.

Another argument for considering the heterolytic fragments as bonding partners has been provided by Dietz et al.[34] They have carried out the only EDA analysis for a pair of cyanide/isocyanide, namely CuCN and CuNC. In their work, they considered both possibilities, the neutral and the charged fragments, concluding that the heterolytic approach is more appropriate to characterize the Cu−CN and Cu−NC bonds. One important argument is that the orbital term from the EDA study is significantly smaller for both cyanide and isocyanide isomers when computed through the heterolytic approach than with the neutral fragments, which means that the relaxation of the wave functions of both isomers releases much less energy when the charged fragments are considered.[34] We have carried out an EDA analysis in terms of homolytic fragments to check whether this argument also holds for the rest of cyanides/isocyanides. Our results are in agreement with the previous study on copper cyanide and isocyanide. Both the NBO charges and the previous analysis on copper cyanide and isocyanide led us to adopt the heterolytic approach. In Figures 2 and 3, the most relevant data from the EDA calculations are provided (the whole set of results from the EDA analysis can be found in Tables S4 and S5 in the Supporting Information). In Figure 2, the electrostatic and orbital contributions for the different cyanide and isocyanide isomers along the transition series are represented, whereas in Figure 3, the σ and π precentage contributions to the orbital term are depicted.

We begin the discussion by commenting on the relative contributions of the electrostatic and orbital terms (Figure 2; see also Tables S4 and S5 in the Supporting Information). We first note that the metal−cyanide/isocyanide bonds are much more electrostatic (about 70−80% of the total attractive interactions) than covalent. It is evident that the relative weight of these terms depends on the choice of the interacting fragments (charged or neutral) and these percentages alone have limited meaning. To put them into perspective, we have performed an EDA calculation on NaCN, whose bond is supposed to have a clear ionic character. This is actually confirmed by the calculation, which shows that attractive interactions are dominated by the electrostatic forces (90.5%), with a marginal 9.5% contribution of the orbital term. The larger orbital contribution found in the transition metal cyanides and isocyanides (about 20−30%) cleary indicates a larger covalent character in these molecules. Notice that the linear structure adopted by all first-row transition metal cyanides can be directly related to these partial covalent character, because the M−C/N covalent bonding mainly occurs through the interaction of the metal 4s/3d$_z^2$ orbitals and the 5σ molecular orbital of CN (NaCN, on the contrary, adopts a T-shape structure[8]). We would like to point out that the nature of the metal−ligand bond does not strongly depend on the metal atom, which in all cases is 70−80% electrostatic.

Regarding the preference for the cyanide or isocyanide conformation, the results collected in Figure 2 show that for the late metals Co−Zn it is the electrostatic term that is clearly larger in MCN than in MNC, whereas the orbital contribution does not change significantly. Thus, the EDA results suggest that late transition metal cyanides are more stable than the isocyanides because of larger electrostatic attractions. This result has been first proposed by Dietz et al.[34] in their study of Cu-

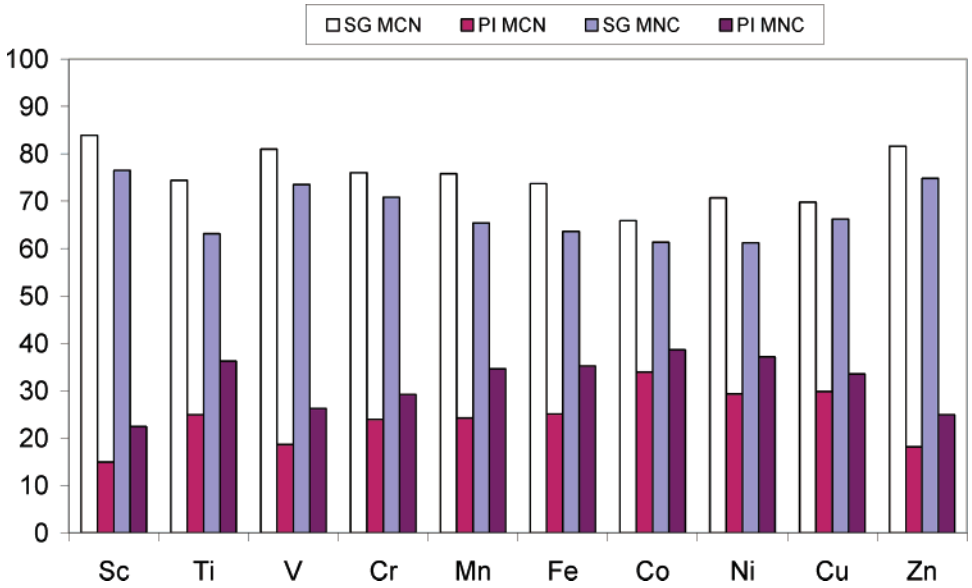

Figure 3. Percentages of the σ and π contributions to the orbital term from the energy decomposition analysis at the BP86/TZ2P+ level of M−CN and M−NC (M = Sc−Zn).

(CN). It can be explained in terms of the shape of the electron density distribution, which shows that the carbon atom has a larger and more diffuse area of charge concentration than nitrogen.[34] Our data suggest that this explanation for the preference of a cyanide conformation can be extended to Co(CN), Ni(CN), and Zn(CN). Notice that these compounds have the shortest metal−ligand bond distance among the transition metal cyanides (see Table 1). Among the early transition metals, the only system for which we found a clear preference for the cyanide conformation was Cr(CN). Figure 2 shows that this is actually an interesting case because electrostatic forces favor again the cyanide, whereas orbital interactions favor the isocyanide conformation approximately in the same amount. The Pauli repulsion term, which is smaller for the cyanide isomer (see Table S4 in the Supporting Information), becomes important, in this case, favoring the cyanide conformation.[73] We would like to stress that for the early transition metals and iron, we find more subtle differences between cyanides and isocyanides. This is also reflected in the smaller relative energies $E_{MNC}-E_{MCN}$ (see Table 3) displayed by early transition metals.

We turn now to Sc(CN) and Ti(CN), which seem to have a clearer preference for the isocyanide isomer. Figure 2 shows that for Sc(CN), there is an increase in both ΔE_{elstat} and ΔE_{orb} in the isocyanide conformation, which is therefore favored because of stronger attractive forces. The same trend is also found in Ti(CN), although the energy differences here are smaller. We stress that for these two compounds, which have the longest metal−ligand bond distance among the first transition row, it is the isocyanide isomer that is favored by the electrostatic forces. This leads us to conclude that the preference for the cyanide isomer in terms of larger electrostatic interactions with the carbon lone pair seems to hold only for metal−ligand bond distances that are short enough. With longer bonds, the overlap between the metal atom and the carbon lone pair reduces and now the electrostatic interaction of the metal with the more negative nitrogen atom could be more favored. Finally, for Mn(CN) and Fe(CN), it seems that orbital interactions favor the isocyanide isomer, because the electrostatic contribution is very similar in the two conformers. For these two compounds and for V(CN), both isomers are found to be nearly isoenergetic (see Table 3) and the final preference for the cyanide or isocyanide conformation is necessarily due to subtle differences among the different contributions to the bonding.

We would also like to comment on the π bonding, because it has been argued[23] that metal → ligand π back-donation may also explain the conformational preference. The argument is the following: because the unoccupied π^* orbitals of CN are more carbon in character, cyanides would be favored over isocyanides when the metal atom has enough dπ electrons to back-donate to the CN moiety.[23] This would be the case of Co(CN), Ni(CN), Cu(CN), and Zn(CN), which all present a cyanide conformation as has been determined by rotational spectroscopy.[22−25] On the other hand, early transition metal (as well as alkaline earth cyanides) are more stable in the isocyanide form because, lacking enough dπ electrons, they prefer to bind the more electronegative nitrogen atom.[23] The importance of the π bonding has been addressed in previous theoretical studies. For example, Nelin et al. concluded, on the basis of population analysis, that there is essentially no π back-bonding in CuCN.[33] Dietz et al. arrived to the same conclusion using an energy decomposition analysis.[34] Besides, Paul et al. argued in their study of NiCN that π bonding should not be very important because both doublet states (with filled dπ orbitals) and quartet states (with partially filled dπ orbitals) have similar C−N bond lengths.[30] Thus, previous theoretical work agree in that π interactions does not seem to play a major role in the metal ligand bonding, at least for late transition metals. To check whether this conclusion can be extended to the whole first transition row, we have collected the NBO populations of the metal dπ orbitals in Table 7. These values, compared with the expected number of dπ electrons of the metal atom from the electronic configuration, clearly show that π donation is indeed not very important for the whole first transition row. The NBO populations also show that for those compounds with filled or partially filled dπ orbitals (from V(CN) to Zn(CN)), π donation takes place mainly in the metal → ligand direction. On the other hand, for the early transition metal cyanides Sc(CN) and Ti(CN), with empty dπ orbitals, π donation takes place in the ligand → metal direction. We address now the question of how much the π bonding contributes to the total bond energy, which can be readily estimated from the EDA analysis. The percentages of the σ and π contributions to the orbital term, collected

in Figure 3, show that π bonding represents about 15−38% of the total orbital ($\sigma + \pi + \delta$) interaction.[74] Notice that this interaction is, in turn, only 20−30% of the total attractive forces, suggesting that in fact π bonding plays only a limited role in the metal−ligand bond. However, the most interesting result we can obtain from the data depicted in Figure 3 is that isocyanides have a larger π character than cyanides for both early and late transition metals. This also holds for the absolute values of the π orbital interactions (collected in Tables S3 and S4), which are always larger for the isocyanides. This result clearly shows that π bonding always favors the isocyanide conformation, regardless of the metal atom, and that π bonding cannot itself explain the conformational preference.

Conclusions

The molecular structure of the first-row transition metal cyanides and isocyanides M(CN) (M = Sc−Zn) has been theoretically studied, providing predictions for their molecular properties. A careful analysis of the competition between cyanide and isocyanide isomers along the transition series has been carried out. The general trend suggested by the theoretical calculations is that early transition metals (Sc−Fe), with the only exception of the Cr(CN) system, favor the isocyanide isomer, whereas late transition metals (Co−Zn) clearly prefer a cyanide arrangement. This general trend is in agreement with the available experimental evidence, which supports a preference for cyanide isomer in CrCN, Co(CN), Ni(CN), Cu(CN), and Zn(CN), whereas for Fe(CN), the experiments have found the isocyanide isomer. Therefore, our theoretical calculations predict the following unknown isocyanides, ScNC($^3\Delta$), TiNC($^4\Phi$), VNC($^5\Delta$), and MnNC($^7\Sigma^+$), as the main targets for experimental detection. However, it must be noted that the relative energy between both isomers is very small, and in some cases (V, Mn), they are nearly isoenergetic. Therefore, a possible experimental characterization of the corresponding cyanides in those cases cannot be discarded.

First-row transition metal cyanides and isocyanides have generally relatively large dissociation energies, with values within the range 80−101 kcal mol^{-1}, except Zn(CN), which has dissociation energies around 50−55 kcal mol^{-1}. The general trend is that the dissociation energy diminishes as one moves from left to right of the row. Therefore, the yet experimentally unknown cyanides/isocyanides seem to be comparatively more stable than most of the observed cyanides/isocyanides.

The isomerization process has also been studied. In all cases, the variation of the energy with the bond angle is rather smooth, and consequently relatively low barriers for the MNC → MCN conversion are found. The largest value is found for V(CN), namely 10.5 kcal mol^{-1} at the CCSD(T) level, but in most cases, the barrier for isomerization is around 3−8 kcal mol^{-1}. These values agree with previous predictions when available (Cu and Fe), and are consistent with a low degree of covalency for the metal−cyanide bond. This feature is confirmed by the topological analysis of the charge density.

A detailed analysis of the bonding has been carried out in terms of an energy decomposition analysis (EDA). This analysis shows that the competition between cyanides and isocyanides for transition metals, with rather small differences in stability, is the result of a delicate balance between the different interactions. Nevertheless, the EDA calculations allows us to detect some interesting trends: (a) the experimentally observed preference for cyanides in the case of late transition metals (Co−Zn) is mainly due to electrostatic interactions, whereas orbital contributions are similar for both cyanides and isocyanides; (b) for the early transition metals Sc and Ti, with longer metal−ligand bond distances, both the electrostatic and the orbital terms favor the isocyanide isomer. For V−Fe, which display intermediate bond distances, the final preference for the cyanide or isocyanide conformation is the result of a delicate balance between the different contributions to the interaction energy; (c) the amount of π donation is small; for late transition metals it takes place from the metal to the ligand, whereas for the early transition metals with empty dπ orbitals, it seems to take place mainly in the opposite direction.

Acknowledgment. This research has been supported by the Ministerio de Educación y Ciencia of Spain (Grant CTQ2004-07405-C02-01) and the Junta de Castilla y León (Grant VA 085/03). V.M.R. gratefully ackowledges funds from the Ministerio de Educación y Ciencia within the Ramón y Cajal Program and cofunding from the Fondo Social Europeo (Programa Operativo Integrado FEDER-FSE, 2000/2006). We thank Dr. I. S. K. Kerkines (Emory University, Atlanta, GA) for helpful comments regarding the multiconfigurational calculations.

Supporting Information Available: Complete refs 47 and 52. Infrared intensities and dipole moments for cyanides and isocyanides (Tables S1 and S2). Geometries of the transition states (Table S3). Data from the energy decomposition analysis (Tables S4 and S5). This material is available free of charge via the Internet at http://pubs.acs.org.

References and Notes

(1) Clementi, E.; Kistenmacher, H.; Popkie, H. *J. Chem. Phys.* **1973**, *58*, 2460.
(2) Torring, T.; Bekooy, J. P.; Meerts, W. L.; Hoeft, J.; Tiemann, E.; Dymanus, A. *J. Chem. Phys.* **1980**, *73*, 4875.
(3) Dorigo, A.; Schleyer, P. v. R.; Hobza, P. *J. Comput. Chem.* **1994**, *15*, 322.
(4) Marsden, C. J. *J. Chem. Phys.* **1982**, *76*, 6451.
(5) Kawaguchi, K.; Kagi, E.; Hirano, T.; Takano, S.; Saito, S. *Astrophys. J.* **1993**, *406*, L39.
(6) Ishii, K.; Hirano, T.; Nagashima, U.; Weis, B.; Yamashita, K. *Astrophys. J.* **1993**, *410*, L43.
(7) Steimle, T. C.; Saito, S.; Takano, S. *Astrophys. J.* **1993**, *410*, L49.
(8) van der Waals, J. J.; Meerts, W. L.; Dymanus, A. *Chem. Phys.* **1984**, *86*, 147.
(9) van der Waals, J. J.; Meerts, W. L.; Dymanus, A. *J. Mol. Spectrosc.* **1984**, *106*, 280.
(10) Robinson, J. S.; Apponi, A. J.; Ziurys, L. M. *Chem. Phys Lett.* **1997**, *278*, 1.
(11) Walker, K. A.; Gerry, M. C. L. *Chem. Phys. Lett.* **1997**, *278*, 9.
(12) Walker, K. A.; Evans, C. J.; Suh, S. H. K.; Gerry, M. C. L.; Watson, J. K. G. *J. Mol. Spectrosc.* **2001**, *209*, 178.
(13) Ziurys, L. M.; Apponi, A. J.; Guelin, M.; Cernicharo, J. *Astrophys. J.* **1995**, *445*, L47.
(14) Highberger, J. L.; Ziurys, L. M. *Astrophys. J.* **2003**, *597*, 1065.
(15) Ziurys, L. M.; Savage, C.; Highberger, J. L.; Apponi, A. J.; Guelin, M.; Cernicharo, J. *Astrophys. J.* **2002**, *564*, L45.
(16) Highberger, J. L.; Savage, C.; Bieging, J. H.; Ziurys, L. M. *Astrophys. J.* **2001**, *562*, 790.
(17) Guelin, M.; Muller, S.; Cernicharo, J.; Apponi, A. J.; McCarthy, M. C.; Gottlieb C. A.; Thaddeus, P. *Astron. Astrophys.* **2000**, *363*, L9.
(18) Guélin, M.; Muller, S.; Cernicharo, J.; McCarthy, M. C.; Thaddeus, P. *Astron. Astrophys.* **2004**, *426*, L49.
(19) Duley, W. W.; Williams, D. A. *Interstellar Chemistry*; Academic Press: London, 1984.
(20) Walmsley, C. M.; Bachiller, R.; Forets, G. P. d.; Schilke, P. *Astrophys. J.* **2002**, *566*, L109.
(21) Lie, J.; Dagdigian, P. J. *J. Chem. Phys.* **2001**, *114*, 2137.
(22) Grotjahn, D. B.; Brewster, M. A.; Ziurys, L. M. *J. Am. Chem. Soc.* **2002**, *124*, 5895.
(23) Brewster, M. A.; Ziurys, L. M. *J. Chem. Phys.* **2002**, *117*, 4853.
(24) Sheridan, P. M.; Ziurys, L. M. *J. Chem. Phys.* **2003**, *118*, 6370.
(25) Sheridan, P. M.; Flory, M. A.; Ziurys, L. M. *J. Chem. Phys.* **2004**, *121*, 8360.

(26) Flory, M. A.; Field, R. W.; Ziurys, L. M. *Mol. Phys.* **2007**, *105*, 585.
(27) Kingston, C. T.; Merer, A. J.; Varberg, T. D. *J. Mol. Spectrosc.* **2002**, *215*, 106.
(28) Boldyrev, A. I.; Li, X.; Wang, L. S. *J. Chem. Phys.* **2000**, *112*, 3627.
(29) Bauschlicher, C. W. *Surf. Sci.***1985**, *154*, 70.
(30) Paul, A.; Yamaguchi, Y.; Schaefer, H. F.; Peterson, K. A. *J. Chem. Phys.* **2006**, *124*, 034310.
(31) DeYonker, N. J.; Yamaguchi, Y.; Allen, W. D.; Pak, C.; Schaefer, H. F.; Peterson, K. A. *J. Chem. Phys.* **2004**, *120*, 4726.
(32) Hirano, T.; Okuda, R.; Nagashima, U.; Spirko, V; Jensen, P. *J. Mol. Spectrosc.* **2006**, *236*, 234.
(33) Nelin, C. J.; Bagus, P. S.; Philpott, M. R. *J. Chem. Phys.* **1987**, 87, 2170.
(34) Dietz, O.; Rayón, V. M.; Frenking, G. *Inorg. Chem.* **2003**, *42*, 4977.
(35) Largo, A.; Redondo, P.; Barrientos, C. *J. Am. Chem. Soc.* **2004**, *126*, 14611.
(36) Rayón, V. M.; Redondo, P.; Barrientos, C.; Largo, A. *Chem.—Eur. J.* **2006**, *12*, 6963.
(37) Becke, A. D. *J. Chem. Phys.* **1986**, *84*, 4524.
(38) Becke, A. D. *J. Chem. Phys.* **1988**, *88*, 2547.
(39) Lee, C.; Yang, W.; Parr, R. G. *Phys. Rev. B* **1988**, *37*, 785.
(40) Becke, A. D. *J. Chem. Phys.* **1988**, *88*, 1053.
(41) Pople, J. A.; Head-Gordon, M.; Raghavachari, K. *J. Chem. Phys.* **1987**, *87*, 5968.
(42) Krishnan, R.; Binkley, J. S.; Seeger, R.; Pople, J. A. *J. Chem. Phys.* **1980**, *72*, 650.
(43) Wachters, A. J. H. *J. Chem. Phys.* **1970**, *52*, 1033.
(44) Hay, P. J. *J. Chem. Phys.* **1977**, *66*, 4377.
(45) Raghavachari, K.; Trucks, G. W. *J. Chem. Phys.* **1989**, *91*, 1062.
(46) Raghavachari, K.; Trucks, G. W.; Pople, J. A.; Head-Gordon, M. *Chem. Phys. Lett.* **1989**, *157*, 479.
(47) Frisch, M. J.; et al. *Gaussian 98*; Gaussian Inc.: Pittsburgh, PA, 1998.
(48) Werner, H.-J.; Knowles, P. J. *J. Chem. Phys.* **1985**, *82*, 5053.
(49) Werner, H.-J.; Knowles, P. J. *Chem. Phys. Lett.* **1985**, *115*, 259.
(50) Werner, H.-J.; Knowles, P. J. *J. Chem. Phys.* **1988**, *89*, 5803.
(51) Werner, H.-J.; Knowles, P. J. *Chem. Phys. Lett.* **1988**, *145*, 514.
(52) Amos, R. D.; et al. *MOLPRO*, 2002.1.
(53) Bader, R. F. W. *Atoms in Molecules. A Quantum Theory*; Clarendon Press: Oxford, 1990.
(54) Popelier, P. L. A. *Comp. Phys. Commun*. **1996**, *93*, 212.
(55) Reed, A. E.; Curtiss, L. A.; Weinhold, F. *Chem. Rev.* **1988**, *88*, 899.
(56) Morokuma, K. *J. Chem. Phys.* **1971**, *55*, 1236.
(57) Morokuma, K. *Acc. Chem. Res.* **1977**, *10*, 294.
(58) Ziegler, T.; Rauk, A. *Theor. Chim. Acta* **1977**, *46*, 1.
(59) Bickelhaupt, F. M.; Baerends, E. J. *Rev. Comput. Chem.* **2000**, *15*, 1.
(60) te Velde, G.; Bickelhaupt, F. M.; Baerends, E. J.; van Gisbergen, S. J. A.; Fonseca Guerra, C.; Snijders, J. G.; Ziegler, T. *J. Comput. Chem.* **2001**, *22*, 931.
(61) Phillips, J. G. *Astrophys. J.* **1973**, *180*, 617.
(62) Frenking, G. *Angew. Chem., Int. Ed.* **2003**, *42*, 3335.
(63) Haaland, A.; Shorokov, D. J.; Tverdova, N. V. *Chem.—Eur. J.* **2004**, *10*, 4416.
(64) Poater, J.; Sola, M.; Bickelhaupt, F. M. *Chem.—Eur. J.* **2006**, *12*, 2902.
(65) Frenking, G.; Esterhuysen, C.; Kovacs, A. *Chem.—Eur. J.* **2006**, *12*, 7773.
(66) Poater, J.; Visser, R.; Sola, M.; Bickelhaupt, F. M. *J Org. Chem.* **2007**, *72*, 1134.
(67) Bader, R. F. W. *Chem. Rev.* **1991**, *91*, 893.
(68) Cremer, D.; Kraka, E. *Angew. Chem., Int. Ed.* **1984**, *23*, 627.
(69) Becke, A. D. *Phys. Rev. A* **1988**, *38*, 3098.
(70) Perdew, J. P. *Phys. Rev. B* **1986**, *33*, 8822.
(71) Snijders, J. G.; Baerends, E. J.; Vernooijs, P. *At. Data Nucl. Data Tables* **1982**, *26*, 483.
(72) Baerends, E. J.; Ellis, D. E.; Ros, P. *Chem. Phys.* **1973**, *2*, 41.
(73) The fact that stronger bonds may come from less Pauli repulsion in addition to stronger attractive interactions has been discussed, for example, in: Esterhuysen, C.; Frenking, G. *Theor. Chem. Acc.* **2004**, *111*, 381−389. Bickelhaupt, F. M.; DeKock, R. L.; Baerends, E. J. *J. Am. Chem. Soc.* **2002**, *124*, 1500−1505.
(74) The δ contribution to the orbital term is always smaller than 2% and is not shown in Figure 3 for the sake of simplicity. We also remind the reader that the orbital interaction is not only due to charge transfer but also to charge polarization of the fragment's density due to the presence of the other fragment.